

## X-RAY OBSERVATIONAL SIGNATURE OF A BLACK HOLE ACCRETION DISC IN AN ACTIVE GALACTIC NUCLEUS RX J1633+4718

W. YUAN<sup>1,2</sup>, B.F. LIU<sup>1,2</sup>, H. ZHOU<sup>3</sup>, T.G. WANG<sup>3</sup>

## ABSTRACT

We report the discovery of a luminous ultra-soft X-ray excess in a radio-loud narrow-line Seyfert 1 galaxy, RX J1633+4718, from archival *ROSAT* observations. The thermal temperature of this emission, when fitted with a blackbody, is as low as  $32.5^{+8.0}_{-6.0}$  eV. This is in remarkable contrast to the canonical temperatures of  $\sim 0.1$ – $0.2$  keV found hitherto for the soft X-ray excess in active galactic nuclei (AGN), and is interestingly close to the maximum temperature predicted for a postulated accretion disc in this object. If this emission is indeed blackbody in nature, the derived luminosity ( $3.5^{+3.3}_{-1.5} \times 10^{44}$  erg s<sup>-1</sup>) infers a compact emitting area with a size ( $\sim 5 \times 10^{12}$  cm or 0.33 AU in radius) that is comparable to several times the Schwarzschild radius of a black hole at the mass estimated for this AGN ( $\sim 3 \times 10^6 M_\odot$ ). In fact, this ultra-steep X-ray emission can be well fitted as the (Compton scattered) Wien tail of the multi-temperature blackbody emission from an optically thick accretion disc, whose parameters inferred (black hole mass and accretion rate) are in good agreement with independent estimates using optical emission line spectrum. We thus consider this feature as a signature of the long-sought X-ray radiation directly from a disc around a super-massive black hole, presenting observational evidence for a black hole accretion disc in AGN. Future observations with better data quality, together with improved independent measurements of the black hole mass, may constrain the spin of the black hole.

*Subject headings:* accretion disks – galaxies: active – galaxies: jets – galaxies: Seyfert – X-rays: galaxies – galaxies: individual (RX J1633+4718)

## 1. INTRODUCTION

Accretion of matter onto a black hole (BH) via an optically thick disc (Shakura & Sunyaev 1973; Novikov & Thorne 1973) is widely accepted as the engine to power active galactic nuclei (AGN) and black hole X-ray binaries (BHXBs) in a bright state. In observation, a search of evidence for BH accretion discs has long been pursued, and one important signature to look for is the predicted characteristic multi-temperature blackbody radiation. For BHXBs (BH masses  $M \sim 10 M_\odot$ ) the bulk of the disc blackbody emission, which has a maximum temperature  $kT_{\max} \sim 0.5$ – $1$  keV, falls within the readily observable X-ray bandpass, and the disc model has proven to be prevailing (see e.g. Done et al. 2007a, for a recent review). In AGNs harbouring super-massive black holes (SMBH) with typical  $M \sim 10^{6-9} M_\odot$  and hence much lower  $T_{\max}$ , however, the situation is much less clear. The main difficulty lies in that the bulk of the disc emission falls within the far-to-extreme UV regime, which is not observable due to Galactic absorption. While it is generally thought that the optical/UV "big blue bump" of AGN is likely associated with disc emission (e.g. Shields 1978; Malkan 1983), some key issues have not been settled yet, however (e.g. Laor et al. 1997).

A long-standing puzzle is that, although the (Compton scattered) Wien tail of the disc blackbody emission is expected to plunge into the soft X-ray band (e.g. Ross et al. 1992; Shimura & Takahara 1995a), convincing evidence remains illusive. Indeed, a soft X-ray excess is commonly detected in AGNs; however, their thermal temperatures, which appear to fall within a narrow range ( $kT \sim 0.1$ – $0.2$  keV), are too high

to conform the disc model prediction (e.g. Gierliński & Done 2004), even with the effects of Compton scattering taken into account (Ross et al. 1992). Neither the inferred luminosities agree with the model values self-consistently (e.g. Miniutti et al. 2009). Furthermore, the independence of temperature on  $M$  found recently argues against the disc blackbody origin (e.g. Bianchi et al. 2009). In general, the soft X-ray excess is suggested to have different origins from disc emission (e.g. Done et al. 2007b). Although there were limited previous attempts to link the soft X-ray excess with disc emission in a few AGNs, e.g. Mkn766 (Molendi et al. 1993) and RE J1034+396 (Puchnarewicz et al. 2001), whereby  $M$  and accretion rates were constrained from the X-ray (and optical/UV) data, the evidence is far from convincing.

In this paper, we report on an ultra-soft X-ray excess detected in an AGN RX J1633+4718, whose thermal temperature ( $kT \sim 30$  eV) is among the lowest ever detected. We show that this emission is well consistent with blackbody radiation from an optically thick accretion disc around a SMBH. We assume a cosmology with  $H_0 = 70$  km s<sup>-1</sup> Mpc<sup>-1</sup>,  $\Omega_M = 0.3$ , and  $\Omega_\Lambda = 0.7$ . Errors are quoted at the 90% confidence level unless mentioned otherwise.

## 2. RX J1633+4718

RX J1633+4718 (SDSS J163323.58+471859.0) was first identified with a narrow-line Seyfert 1 (NLS1) galaxy at a redshift  $z=0.116$  in optical identification of the *ROSAT* All-Sky Survey (RASS) sources (Moran et al. 1996; Wisotzki & Bade 1997). The AGN resides in one of a pair of galaxies, with the other a starburst galaxy separated by 4'' (Bade et al. 1995). It is associated with a variable, invert spectrum radio source (Neumann et al. 1994) with an unresolved VLBI core at milli-arcsec resolution (Doi et al. 2007). It is among a very radio-loud NLS1 AGN sample studied by Yuan et al. (2008). This rare type of AGNs exhibit properties characteristic of blazars, i.e. having relativistic jets directed close to the line-of-sight (Zhou et al. 2007; Yuan et al. 2008), which has been con-

Electronic address: wmy@ynao.ac.cn

<sup>1</sup> National Astronomical Observatories/Yunnan Observatory, Chinese Academy of Sciences, Kunming, Yunnan, P.O. BOX 110, China<sup>2</sup> Key Laboratory for the Structure and Evolution of Celestial Objects, Chinese Academy of Sciences<sup>3</sup> Key Laboratory for Research in Galaxies and Cosmology, Center for Astrophysics, University of Science and Technology of China, Hefei, Anhui, China

firmed in several of the objects by recent  $\gamma$ -ray observations with *Fermi* (Abdo et al. 2009).

Its optical spectrum, acquired in the Sloan Digital Sky Survey (SDSS) and analysed in Yuan et al. (2008, see their Figure 1), has broad components of the  $H\beta$  and  $H\alpha$  lines with a width  $FWHM = 909 \pm 43 \text{ km s}^{-1}$  and a luminosity  $3.14(11.7) \times 10^{41} \text{ erg s}^{-1}$ , respectively. The expected "thermal" continuum luminosity at 5100 *estimated from the  $H\beta$  luminosity* is  $\lambda L_{\lambda 5100} = 2.63 \times 10^{43} \text{ erg s}^{-1}$  using the relations from Greene & Ho (2005). The "thermal" bolometric luminosity (i.e. free from the non-thermal jet emission) can then be estimated as  $L_{\text{bol}} = k \lambda L_{\lambda 5100} = 2.6(\pm 0.5) \times 10^{44} \text{ erg s}^{-1}$ , adopting  $k = 10 \pm 2$  ( $1\sigma$ ) for *radio-quiet* AGNs (Richards et al. 2006). The BH mass, estimated from the broad Balmer linewidth and the luminosity of either the broad line or the "thermal" continuum lies within  $M \simeq 2.0 - 3.5 \times 10^6 M_{\odot}$  using various commonly adopted formalisms (e.g. Vestergaard & Peterson 2006; Collin et al. 2006; Greene & Ho 2007). We thus adopt a nominal value  $M = 3 \times 10^6 M_{\odot}$ , with a systematic uncertainty of  $\sim 0.3$  dex (Vestergaard & Peterson 2006). The estimated Eddington ratio is then  $L/L_{\text{Edd}} = 0.69^{+0.73}_{-0.35}$ , using the above "thermal" bolometric luminosity.

### 3. ULTRA-SOFT X-RAY EXCESS EMISSION

J1633+4718 was observed with the ROSAT PSPC-b on axis with a 3732 s exposure on July 24th, 1993, and also detected during the RASS (PSPC-c) with a weighted exposure of 909 s. The reduction and a brief analysis of the ROSAT data was presented in Yuan et al. (2008). To summarise, there are  $\sim 976$  net source counts in the pointed observation and 185 counts in the RASS. The 0.1–2.4 keV spectrum can be well modeled with two components, an ultra-soft X-ray component dominating energies below 0.4 keV and a flat power-law (photon index  $\Gamma \sim 1.37$ ) dominating energies above 0.4 keV; the latter was interpreted as inverse Compton emission from a relativistic jet (Yuan et al. 2008). In this paper we focus on the ultra-soft X-ray component and revisit the spectrum by performing a more detailed analysis.

We use the pointed observation spectrum (Figure 1) to derive spectral parameters, given its much higher data signal-to-noise ratio (S/N) than that of the RASS data. *XSPEC* (v.12.5) is used to perform spectral fit. Neutral absorption with a  $H\text{I}$  column density  $N_{\text{H}}$  is always added in spectral models concerned. The Galactic  $N_{\text{H}}^{\text{Gal}} = 1.79 \times 10^{20} \text{ cm}^{-2}$  on the line-of-sight, measured from the LAB Survey (Kalberla et al. 2005). The results are summarised in Table 1. We first try a simple power-law model. The fit is unacceptable for fixing  $N_{\text{H}} = N_{\text{H}}^{\text{Gal}}$  ( $\chi^2/\text{d.o.f.} = 67/30$ ), underestimating severely the fluxes at both the low and high energies. Setting  $N_{\text{H}}$  free still yields a poor fit, since the same systematic structures remain in the residuals and, even worse, resulting in little or no absorption. Fitting the higher-energy (0.4–2.4 keV) spectrum only (fixing  $N_{\text{H}} = N_{\text{H}}^{\text{Gal}}$ ) yields a good fit and a flat  $\Gamma = 1.63(\pm 0.4)$ , while extrapolating this power-law to lower energies reveals a prominent soft X-ray excess, as shown in Figure 1 (middle panel).

Therefore an additional emission component is added to account for the soft X-ray excess, that is modeled by commonly adopted models including blackbody, power-law, thin plasma and thermal bremsstrahlung. In general, all these models yield nearly the same excellent fits and the systematic structures in the residuals vanish. However, they cannot be distinguished based on fitting statistics. For most of the models, and particularly blackbody, the fitted  $N_{\text{H}}$  values are in good agreement with  $N_{\text{H}}^{\text{Gal}}$ , albeit large uncertainties. We thus fix the absorp-

tion  $N_{\text{H}} = N_{\text{H}}^{\text{Gal}}$  when deriving spectral parameters (Table 1). As an example, the best-fit power-law plus blackbody model and the residuals are shown in Figure 1. We note that the addition of a second, relatively steep power-law continuum as in normal Seyferts with fixed  $\Gamma = 2-3$  is not required, indicating that it is negligible.

Interestingly, the fitted (rest frame) thermal temperatures are surprisingly low, e.g.  $kT_{\text{bb}} = 32.5^{+8.0}_{-6.0} \text{ eV}$  for a (redshifted) blackbody. Such an exceptionally low temperature is in remarkable contrast to the "canonical"  $\sim 0.1-0.2 \text{ keV}$  found for AGNs (Gierliński & Done 2004; Haba et al. 2008; Bianchi et al. 2009), and is perhaps the lowest with confident measurement known so far<sup>4</sup> (to our knowledge). In fact, the ultra-softness of this component is evident, as it dominates the emission below 0.4 keV only. The *overall* blackbody luminosity is high,  $L_{\text{bb}} = 3.5^{+3.3}_{-1.5} \times 10^{44} \text{ erg s}^{-1}$ , whose confidence contours vs.  $kT_{\text{bb}}$  are shown in Figure 2. In fact, the blackbody luminosity is comparable to the "thermal" bolometric luminosity [ $\sim 2.8(\pm 0.6) \times 10^{44} \text{ erg s}^{-1}$ ], which is remarkable considering the large uncertainty in the bolometric correction. Hence we assume this ultra-soft X-ray emission as blackbody in nature.

The spectrum measured in the RASS has an almost identical spectral shape as that of the pointed observation. The best-fit parameters are in excellent agreement with those obtained from the pointed observation, with  $\Gamma = 1.47^{+0.77}_{-0.92}$  and the blackbody temperature  $30^{+12}_{-10} \text{ eV}$  (90% confidence level), though the errors are large given the small source counts. The overall blackbody luminosity is found to be  $3.4 \times 10^{44} \text{ erg s}^{-1}$ . There appears to be no detectable variation in either the spectral shape or the luminosity between the RASS and pointed observation.

### 4. EMISSION FROM AN ACCRETION DISC?

#### 4.1. Size and temperature of X-ray emitting region

Assuming blackbody radiation, the size of the emitting area can be inferred as  $A = L_{\text{bb}}/(\sigma T_{\text{bb}}^4)$  ( $\sigma$  the Stefan-Boltzmann constant). For an assumed geometry of a sphere or a face-on disc, a radius  $\sim 5(\text{or } 7) \times 10^{12} \text{ cm}$  ( $\sim 0.3-0.5 \text{ AU}$ ) is inferred, which is extremely compact for its high luminosity. In fact, these radii are merely several to ten times the Schwarzschild radius of a BH at the mass estimated for RX J1633+4718 ( $R_{\text{s}} = 2GM/c^2 \approx 9 \times 10^{11} \text{ cm}$ ). An immediate conclusion is that the soft X-ray emitting region must be extremely compact, e.g. most likely in the close vicinity of the central BH.

In the standard BH accretion disc model the local effective temperature at a radius  $R$  is

$$T_{\text{eff}}(R) = \left[ \frac{3GM\dot{M}}{8\pi\sigma R^3} \left( 1 - \sqrt{\frac{R_{\text{in}}}{R}} \right) \right]^{1/4} \quad (1)$$

$$= 6.24 \times 10^5 \left( \frac{R}{R_{\text{s}}} \right)^{-3/4} \left( 1 - \sqrt{\frac{R_{\text{in}}}{R}} \right)^{1/4} \left( \frac{M}{10^8 M_{\odot}} \right)^{-1/4} \dot{m}^{1/4} (\text{K})$$

(Frank et al. 1992; Kato et al. 2008), where  $R_{\text{in}}$  is the radius of the inner boundary (assumed to be the last marginally stable orbit) of the disc, and  $\dot{m} \equiv \dot{M}/\dot{M}_{\text{Edd}}$  the scaled accretion rate, with the Eddington rate defined as  $\dot{M}_{\text{Edd}} \equiv L_{\text{Edd}}/(\eta c^2)$ , e.g.  $1.39 \times 10^{18} M/M_{\odot} \text{ g s}^{-1}$  assuming  $\eta = 0.1$ . For a non-rotating

<sup>4</sup> Lower  $kT$  in a few objects were reported by Urry et al. (1989) based on *Einstein* IPC+MPC data; however, they were not confirmed in latter observations, e.g. in Mkn 766 (Molendi et al. 1993).

BH ( $R_{\text{in}} = 3R_s$ ), from outer part inwards  $T$  reaches its maximum

$$T_{\text{max}} = 11.5 \left( \frac{M}{10^8 M_\odot} \right)^{-1/4} \dot{m}^{1/4} \text{ (eV)}, \quad (2)$$

at  $R = (49/36) \times 3R_s$ , and decreases again inwards. For  $M = 3 \times 10^6 M_\odot$  and assuming  $\dot{m}$  as  $L/L_{\text{Edd}}$  ( $=0.69$ ), we find  $kT_{\text{max}} = 25.3 \text{ eV}$ , that is close to the fitted  $T_{\text{bb}} = 32.5^{+8.0}_{-6.0} \text{ eV}$ . To our knowledge, this is by far the most convincing case where the soft X-ray excess temperature is well compatible with the predicted maximum disc temperature.

#### 4.2. Accretion disc model fit

##### 4.2.1. Standard accretion disc model and parameters

We fit the spectrum with the commonly adopted multi-colour disc (MCD, *diskbb* in *XSPEC*) model (Mitsuda et al. 1984; Makishima et al. 1986). This model has been widely used in fitting the X-ray spectra of BHXBs, and found to provide reasonably good descriptions to the observed spectra at the high/soft state (e.g. Dotani et al. 1997; Kubota et al. 1998). With an approximation to the boundary condition, the MCD model has a monotonic temperature profile,  $T_{\text{eff}}(R) = T_{\text{in}}(R/R_{\text{in}})^{-3/4}$ , where  $T_{\text{in}}$  is the effective temperature at the disc inner radius  $R_{\text{in}}$ . This model should be sufficient for our purpose here, considering the moderate spectral S/N and resolution and the limited bandpass of the PSPC data.

The emergent MCD spectrum is determined by two parameters: the (apparent) radius of the inner boundary of the disc  $R'_{\text{in}}$  and the maximum (colour) temperature  $T'_{\text{in}}$ , which are related to the disc luminosity via

$$L = 4\pi R_{\text{in}}^2 \sigma T_{\text{in}}^4. \quad (3)$$

$T'_{\text{in}}$  and  $R'_{\text{in}} \sqrt{\cos \theta}$  can be derived from spectral fitting, where  $\theta$  is the disc inclination angle. Since the MCD model does not incorporate the redshift effect, which is small for RX J1633+4718 at  $z=0.116$  though,  $T'_{\text{in}}$  and  $R'_{\text{in}}$  in the object's rest frame are obtained by multiplying the fitted values with  $(1+z)$  and  $1/(1+z)$  (can be shown by using Eq. 3), respectively. The true inner boundary radius  $R_{\text{in}}$  is related to the apparent radius  $R'_{\text{in}}$  via  $R_{\text{in}} = \xi R'_{\text{in}}$ , where  $\xi = \sqrt{3/7}(6/7)^3 \approx 0.41$  is introduced to account for the inner boundary condition that is neglected in the MCD model (Kubota et al. 1998; Kato et al. 2008).

The disc inclination  $\theta$  is expected to be a small angle given the blazar-like property of RX J1633+4718, i.e. generally  $\lesssim 10^\circ$  assuming disc-jet perpendicularity. In fact, for a wider range of  $\theta$ , say  $\theta < 30^\circ$  (as expected for type 1 AGNs), the dependence of  $\sqrt{\cos \theta}$  on  $\theta$  is weak. We thus expect  $\sqrt{\cos \theta} \approx 1$ , and hence  $R_{\text{in}} \sqrt{\cos \theta} \approx R_{\text{in}}$ .

To relate the observed spectrum to the true disc parameters corrections should be made to account for the spectral hardening effect, which gives rise to a shifted Wien spectrum to a higher colour temperature due to incoherent Compton scattering (Czerny & Elvis 1987; Wandel & Petrosian 1988; Ross et al. 1992; Shimura & Takahara 1995a). The true effective  $T_{\text{max}}$  is then

$$T_{\text{max}} = \frac{1}{\kappa} T'_{\text{in}}, \quad (4)$$

where  $\kappa$  is the spectral hardening factor. Consequently, the true inner boundary radius

$$R_{\text{in}} = \kappa^2 \xi R'_{\text{in}} \quad (5)$$

(Kato et al. 2008; Kubota et al. 1998). The value of  $\kappa$  is somewhat uncertain, and  $\kappa \simeq 1.7 \pm 0.2$  was suggested (Shimura & Takahara 1995b) based mostly on consideration of BHXBs and  $1 < \kappa \lesssim 2.5$  for SMBHs with wide ranges of  $M$  and  $\dot{m}$  (Ross et al. 1992; Shimura & Takahara 1995a). Here we adopt  $\kappa \simeq 1.7$ .

##### 4.2.2. Results of accretion disc model fit

The spectrum is well fitted with the MCD plus a power-law model, with the fitted  $N_{\text{H}}$  consistent with  $N_{\text{H}}^{\text{Gal}}$ . Fixing  $N_{\text{H}} = N_{\text{H}}^{\text{Gal}}$  yields the same excellent fit as using blackbody, giving  $kT'_{\text{in}} = 39.6^{+12.3}_{-7.5} \text{ eV}$  and  $R'_{\text{in}} = 3.0^{+2.9}_{-1.4} \times 10^{12} / \sqrt{\cos \theta} \text{ cm}$  in the object's rest frame (Table 1). Applying the corrections in Eqs. 4 and 5 with  $\kappa \simeq 1.7$ , we find a true maximum effective temperature  $kT_{\text{max}} = 23.3^{+7.2}_{-4.4} \text{ eV}$  and an inner disc radius  $R_{\text{in}} = 3.6^{+3.4}_{-1.7} \times 10^{12} / \sqrt{\cos \theta} \text{ cm}$ . The confidence contours of  $kT_{\text{max}}$  and  $R_{\text{in}}$  are shown in Figure 3.

Assuming a non-rotating BH and  $R_{\text{in}} = 3R_s$ , we can derive its mass from X-rays,  $M_x$ , and in turn  $\dot{m}$  using  $T_{\text{max}}$  and Eq. 2. We find the best estimates  $M_x = 4.1 \times 10^6 / \sqrt{\cos \theta} M_\odot$  and  $\dot{m} = 0.68 / \sqrt{\cos \theta}$ . The contours of confidence intervals for  $M$  and  $\dot{m}$ , as derived from those of  $R_{\text{in}}$  and  $T_{\text{max}}$  assuming  $\theta = 10^\circ$ , are shown in Figure 3 (right panel). It is interesting to note that the X-ray spectrum provides relatively tight constraint on accretion rate  $\dot{m}$ . This is because the uncertainties of the derived  $R_{\text{in}}$  ( $M_x$ ) and  $T_{\text{max}}$ , albeit large, are highly inversely coupled (left panel) and hence largely canceled mutually.

These derived parameter values can be compared with those estimated from the optical spectrum,  $M$  and  $L/L_{\text{Edd}}$  (assumed as  $\dot{m}$ ), and in turn  $R_{\text{in}}$  and  $T_{\text{max}}$  (using Eq. 2 and assuming  $R_{\text{in}} = 3R_s$ ). Their best estimates and uncertainty ranges are overplotted in Figure 3, as  $\pm 0.3 \text{ dex}$  in  $M$  (Vestergaard & Peterson 2006) and  $\pm 2(1\sigma)$  in the bolometric correction (Richards et al. 2006). Remarkably, the results derived from the X-ray and optical observations agree strikingly well, albeit the relatively large uncertainties in both the measurements. This conclusion is basically not affected by the exact value of  $\kappa$ , provided  $1 \lesssim \kappa \lesssim 2.5$ .

We note that the MCD model is only approximately correct since no general relativistic (GR) effects are taken into account. We make further corrections to the derived disc parameters due to the GR effects following the approach of Zhang et al. (1997). Eqs. 4 and 5 are then  $T_{\text{max}} = f^{-1}(\kappa^{-1} T'_{\text{in}})$  and  $R_{\text{in}} = g^{-0.5} f^2(\kappa^2 \xi R'_{\text{in}})$ , where  $f$  and  $g$  are temperature and flux correction factors, respectively. For a non-rotating BH and  $\theta \approx 0^\circ$ ,  $f \approx 0.85$  and  $g \approx 0.80$  (Zhang et al. 1997, their Table 1). Therefore the above  $kT_{\text{max}}$  and  $R_{\text{in}}$  ( $M_x$ ) values should be further multiplied by a factor of 1.17 and 0.81, respectively, i.e.  $kT_{\text{max}} = 27 \text{ eV}$ ,  $R_{\text{in}} \sim 2.9 \times 10^{12} \text{ cm}$ ,  $M_x \sim 3.3 \times 10^6 M_\odot$ , and  $\dot{m} \sim 1.0$ . These parameter values are still marginally consistent with those derived from the optical spectrum (Figure 3).

Therefore, we conclude that we might be seeing the direct X-ray emission from an accretion disc around the SMBH in RX J1633+4718, which has been long sought for AGNs. We note that, however, for a more realistic modeling, a relativistic disc model taking the GR effects fully into account should be used (such as the *kerrbb* model of Li et al. 2005). Besides, we did not consider the BH spin here, that is also plausible; e.g. for a spinning BH and a prograde disc,  $R_{\text{in}}$  would extend further inwards within  $3R_s$ , i.e.  $R_{\text{in}} < 3R_s$ , and  $T_{\text{max}}$  increases, resulting in an increased  $M_x$  and a reduced  $\dot{m}$ . Furthermore, since the above found  $\dot{m} > 0.3$ , the effects of a slim disc (Abramowicz et al. 1988; Sadowski 2009; Li et al. 2010,



see Chapter 10 of Kato et al. 2008 for a review) may start to set in. We defer all these comprehensive treatments to future work, in a hope that it may shed light on the spin of the BH.

## 5. DISCUSSION

### 5.1. Compatibility with lower-frequency data

Having established the accretion disc emission model from the soft X-ray spectrum, it would be interesting to check whether this model is compatible with the observed broad-band spectral energy distribution (SED) of RX J1633+4718. The unfolded PSPC spectrum and the fitted MCD plus power-law model (dotted line) are shown in Figure 4, along with the broad-band SED whose low-energy data are collected from the NASA/IPAC Extragalactic Database (NED). Interestingly, while the UV-to-infrared spectrum steepens towards lower frequencies, the *Galex* far-UV measurement (squares) agrees roughly with the MCD model prediction. The lack of an obvious big-blue-bump in optical-UV supports that it is likely shifted to higher frequencies. As for the optical-infrared bump, we interpret it as the high-energy tail of beamed synchrotron emission from the relativistic jets, in light of the blazar-like property of RX J1633+4718. We model this component with a parabolic function, a commonly used approximation to the synchrotron emission of blazars. The sum of this model and the above best-fit MCD model is fitted to the radio 5 GHz, near-IR and optical/UV data, excluding the far-IR measurements from *IRAS* and *ISO* (crosses; since they are most likely seriously contaminated, or even dominated by thermal emission of dust<sup>5</sup> from the companion starburst galaxy 4'' away given the relatively poor spatial resolution of *IRAS* and *ISO*). As can be seen, such a synchrotron component (dashed line) can generally account for the SED at lower energies. Therefore, the above accretion disc model, together with the other two emission components (synchrotron and inverse-Compton), is compatible with the observed broad-band SED of RX J1633+4718. Moreover, the lack of detectable variation of the ultra-soft X-ray emission between the RASS and pointed observations also supports the accretion disc model, since the thermal emission from an accretion disc is generally stable over such a relatively short timescale.

We note that the starburst companion must fall within the source extraction region on the PSPC detector plane due to its low spatial resolution. Starburst also produces soft X-rays, which are related to the far-IR luminosity as  $L_{\text{FIR}}^{\text{SB}}/L_{0.3-2\text{keV}} = 10^{3-4}$ . For the companion starburst galaxy, an upper limit on  $L_{\text{FIR}}^{\text{SB}}$  can be set by the *IRAS* measurements using  $f_{100\mu} = 1.12 \text{ Jy}$  and  $f_{60\mu} = 0.595 \text{ Jy}$  (Sanders & Mirabel 1996), yielding  $L_{\text{FIR}}^{\text{SB}} < L_{\text{FIR}} = 3.0 \times 10^{11} L_{\odot}$  ( $1.15 \times 10^{45} \text{ erg s}^{-1}$ ). This corresponds to an upper limit on the soft X-ray luminosity arising from the starburst  $L_{0.3-2\text{keV}}^{\text{SB}} < 1 \times 10^{41-42} \text{ erg s}^{-1}$  only. Such a contribution, if any, would be overwhelmed by the X-ray emission from the AGN given the observed luminosity  $L_{0.3-2\text{keV}} \sim 10^{44} \text{ erg s}^{-1}$ . Moreover, the thermal temperatures of X-ray gases of starburst fall within a strict range of 0.3–0.7 keV, far higher than the fitted 50 eV for a thin plasma model (Table 1). We thus conclude that the *ROSAT* spectrum of RX J1633+4718 is essentially not affected by any potential contamination from the starburst companion.

### 5.2. Why is RX J1633+4718 different from other AGNs?

An interesting question arises as to why RX J1633+4718 is so special and unique, in terms of previous unsuccessful attempts to ascribe the soft X-ray excess (with the canonical temperatures of  $\sim 0.1\text{--}0.2 \text{ keV}$ ) to the direct thermal emission of the accretion discs in the vast majority of AGNs. This question will not be answered until the origin of the puzzling soft X-ray excess in many other AGNs is understood. Nonetheless, we discuss some possibilities here, albeit somewhat speculative. In any case, one important feature of RX J1633+4718 is its dominance of the disc thermal emission, which is a close analogue to the typical high/soft state in BHXBs (relatively weak corona; see above). This is different from many other AGNs in which the soft excess was investigated, where the spectral state is characterised by strong corona emission.

One of the viable explanations of the soft excess is Comptonisation of soft photons (e.g. from discs) off a region with electron temperature  $kT_e \sim 0.1\text{--}0.2 \text{ keV}$  and a large optical depth  $\tau \sim 20$  (e.g. Czerny & Elvis 1987; Gierliński & Done 2004; Done et al. 2007b). In this scenario, RX J1633+4718 may differ from the other AGNs in its environment surrounding the central engine, i.e. lacking this Comptonisation region and the disc being directly seen in the line-of-sight, which may not be the case for the other AGNs. For instance, the difference may be due to the presence of jets (and the face-on inclination of the disc) in RX J1633+4718. It may be possible that in radio-quiet AGNs the Comptonisation region is formed by aborted jets (Henri & Petrucci 1997; Ghisellini et al. 2004) whose kinetic energy is converted to internal energy to heat electrons to the required temperature. In the case of RX J1633+4718, the jets are successfully launched, however, clearing the way to the central disc along the line-of-sight. It is interesting to note that in 3C 273, a well-known AGN with relativistic jets, a relatively low blackbody temperature of the soft excess was also reported ( $\sim 60 \text{ eV}$ ; Grandi & Palumbo 2004; although in that work the accretion disc origin was not tested in terms of matching the X-ray data with the predicted temperature and luminosity of the disc, as we did here). Whether or not this can be generalised to other radio-loud AGNs needs further investigations, though it should be reminded that the jets of radio-loud NLS1s might be different from those of classical radio quasars, e.g. with reduced physical size and power (Yuan et al. 2008).

An alternative model is disk reflection in which the observed soft X-ray excess can be explained as relativistically blurred line emission of the reflection component from a highly ionized inner disc, that somehow dominates the primary emission (Ross & Fabian 1993; Ballantyne et al. 2001; Miniutti & Fabian 2004; Crummy et al. 2006). The postulation of this model is the presence of the primary X-ray emission, presumably from a disc corona of high-temperature and low-optical depth. It may be possible that in RX J1633+4718 the disc corona is significantly suppressed somehow, for instance, due to the formation of the jets (the energy goes into the jets instead of to the corona) or to the relatively high mass accretion rate. This would lead to a weak reflection component in RX J1633+4718 and thus has no significant soft excess in the usual form, while the disc thermal emission stands out. In this line, as mentioned above, the Seyfert-like X-ray component in the *ROSAT* spectrum of RX J1633+4718 is too weak to be detected.

Finally, for AGNs with high black hole masses ( $M > 10^7 M_{\odot}$ ) and relatively low accretion rates, even if the other conditions (jets, corona, etc.) resemble those of

<sup>5</sup> The observed  $f(60\mu)/f(100\mu)=0.53$  is "infrared warm", typical of starburst in the local universe (Soifer et al. 1987).

RX J1633+4718, the thermal disc emission may have too low temperatures to be detectable above the low-energy cutoff of commonly used X-ray detectors ( $\sim 0.1$  keV). Future observations of more AGNs similar to RX J1633+4718 may shed light on under what conditions the direct thermal emission of accretion discs can be detected in X-ray.

## 6. CONCLUDING REMARKS

We have shown that the ultra-soft X-ray excess discovered in RX J1633+4718 can be well and self-consistently described by thermal emission from an optically thick accretion disc around a SMBH. The derived parameters ( $M_X$ ,  $\dot{m}$ , and  $T_{\max}$ ) agree with the independent estimates based on the optical spectrometric data. We thus consider this emission as a signature of X-rays from an accretion disc around a SMBH, presenting possible evidence for BH accretion discs in AGNs. As such, RX J1633+4718 is an AGN analog of BHBs at the high/soft state in a sense that the accretion disc emission dominates the bolometric luminosity. More importantly, one may infer the spin of the BH, as succeeded in BHBs (e.g. Zhang et al. 1997; McClintock et al. 2006). This may be

achieved with future improved observations, which, if successful, would provide a testbed for studying the link of BH spin and the formation of relativistic jets in AGNs. Finally, it is intriguing why RX J1633+4718 is so unique among the many AGNs observed in the soft X-rays, which may be addressed with future investigations.

WY thanks S. Mineshige, A.C. Fabian, and R. Taam for reading the manuscript and providing helpful comments, and F. Meyer and E. Meyer-Hofmeister for discussion, as well as L.M. Dou and X.B. Dong for help with some of the data preparation. This work is supported by NSFC grants 10533050, 10773028, the National Basic Research Program of (973 Program) 2009CB824800. This research has made use of the ROSAT all-sky survey data and pointed observation data which have been processed at MPE. This research has made use of the SDSS data, and the NASA/IPAC Extragalactic Database (NED) which is operated by the Jet Propulsion Laboratory, California Institute of Technology, under contract with the National Aeronautics and Space Administration.

## REFERENCES

- Abramowicz, M.A., Czerny, B., Lasota, J.P., & Szuszkiewicz, E. 1988, *ApJ*, 332, 646
- Abdo A.A., et al. 2009, *ApJ*, 707, L142
- Bade, N., Fink, H.H., Engels, D., Voges, W., Hagen, H.-J., et al., 1995, *A&AS*, 110, 469
- Ballantyne, D.R., Ross, R.R., Fabian, A.C. 2001, *MNRAS*, 327, 10
- Bianchi, S., Guainazzi, M., Matt, G., Fonseca Bonilla, N., & Ponti, G. 2009, *A&A*, 495, 421
- Collin, S., Kawaguchi, T., Peterson, B.M., Vestergaard, M. 2006, *A&A*, 456, 75
- Crummey, J., Fabian, A.C., Gallo, L., & Ross, R.R. 2006, *MNRAS*, 365, 1067
- Czerny, B. & Elvis, M., 1987, *ApJ*, 321, 305
- Doi, A., et al. 2007, *PASJ*, 59, 703
- Done, C., Gierliński, M., Kubota, A., 2007a, *A&ARv*, 15, 1
- Done, C., et al., 2007b, *ASP Conference Series*, Vol. 373, Eds. Ho, L.C. & Wang, J.M., p.121
- Dotani, T., et al. 1997, *ApJ*, 485, L87
- Frank, J., King, A. & Raine, D., 1992, "Accretion Power in Astrophysics", 2nd ed., Cambridge Univ. Press
- Ghisellini, G., Haardt, F. & Matt, G. 2004, *A&A*, 413, 535
- Gierliński, M. & Done, C. 2004, *MNRAS*, 349, 7
- Grandi, P. & Palumbo, G.G.C. 2004, *Science*, 306, 998
- Greene, J.E. & Ho, L.C. 2005, *ApJ*, 630, 122
- Greene, J.E. & Ho, L.C. 2007, *ApJ*, 670, 9
- Haba, Y., Terashima, Y., Kunieda, H., Ohsuga, K., 2008, *ASR*, 41, 174
- Henri, G. & Petrucci, P.O. 1997, *A&A*, 326, 87
- Kalberla, P.M.W., Burton, W.B., Hartmann, D., Arnal, E.M., Bajaja, E., et al. 2005, *A&A*, 440, 775
- Kato, S., Fukue, J., Mineshige, S. 2008, "Black hole accretion disks", 2nd ed., Kyoto University Press
- Kawaguchi, T. 2003, *ApJ*, 593, 69
- Kubota, A., Tanaka, Y., Makishima, K., Ueda, Y., Dotani, T., et al. 1998, *PASJ*, 50, 667
- Laor, A., Fiore, F., Elvis, M., Wilkes, B.J., McDowell, J.C., 1997, *ApJ*, 477, 93
- Li, G.-X., Yuan, Y.-F., Cao, X., 2010, *ApJ*, 715, L623
- Li, L.-X., et al. 2005, *ApJS*, 157, 335
- Makishima, K., Maejima, Y., Mitsuda, K., Bradt, H.V., Remillard, R.A., et al. 1986, *ApJ*, 308, 635
- Malkan, M., 1983, *ApJ*, 268, 582
- McClintock, J., et al., 2006, *ApJ*, 652, 518
- Miniutti, G. & Fabian A.C. 2004, *MNRAS*, 349, 1435
- Miniutti, G., Ponti, G., Greene, J. E., Ho, L. C., Fabian, A. C., & Iwasawa, K., 2009, *MNRAS*, 394, 443
- Mitsuda, K., Inoue, H., Koyama, K., Makishima, K., Matsuoka, M., et al. 1984, *PASJ*, 36, 741
- Molendi, S., Maccacaro, T., Schaeidt S., 1993, *A&A*, 271, 18
- Moran, E.C., Halpern, J.P., Helfand, D.J. 1996, *ApJS*, 106, 341
- Neumann, M., Reich, W., Furst, E., Brinkmann, W., Reich, P., et al. 1994, *A&AS*, 106, 303
- Novikov, I.D. & Thorne, K.S., 1973, in "Black Holes", eds de Witt, C. & de Witt, B., Gordon & Breach, New York, p.422
- Puchnarewicz E.M., et al., 2001, *ApJ*, 550, 644
- Richards G.T., et al. 2006, *ApJS*, 166, 470
- Ross, R.R., Fabian, A.C., Mineshige, S., 1992, *MNRAS*, 258, 189
- Ross, R.R., & Fabian, A.C., 1993, *MNRAS*, 261, 74
- Sanders, D.B. & Mirabel, I.F. 1996, *ARA&A*, 34, 749
- Sadowski, A. 2009, *ApJS*, 183, 171
- Shakura, N.I. & Sunyaev R.A. 1973, *A&A*, 24, 337
- Shields, G.A., 1978, *Nature*, 272, 706
- Shimura, T. & Takahara, F. 1995a, *ApJ*, 440, 610
- Shimura, T. & Takahara, F. 1995b, *ApJ*, 445, 780
- Soifer, B.T., et al. 1987, *ApJ*, 320, 238
- Urry, C.M., et al. 1989, in: *proceed. 23rd ESLAB Symp. on Two Topics in X-ray Astronomy*, Bologna, 975
- Vestergaard, M. & Peterson, B.M. 2006, *ApJ*, 641, 689
- Wandel, A. & Petrosian, V. 1988, *ApJ*, 329, L11
- Wisozki, L. & Bade, N. 1997, *A&A*, 320, 395
- Yuan, W., Zhou, H.Y., Komossa, S., Dong, X.B., Wang, T.G., Lu, H.L., Bai, J.M., 2008, *ApJ*, 685, 801
- Zhang, S.N., Cui, W., & Chen, W. 1997, *ApJ*, 482, L155
- Zhou, H.Y., Wang, T.G., Yuan, W., Shan H.G., Komossa, S., et al. 2007, *ApJ*, 658, L13

TABLE 1  
RESULTS OF SPECTRAL FITS

wabs * model <sup>a</sup>	$N_{\text{H}}(10^{20} \text{ cm}^{-2})$	$\Gamma$	$kT(\text{eV}) / \Gamma_s^b$	$\chi^2/\text{d.o.f.}$
powl	$0.37^{+0.30}_{-0.25}$	$2.22^{+0.22}_{-0.20}$		34.1/29
powl	1.79(fixed) <sup>c</sup>	3.06		67.4/30
powl (0.4–2.4 keV)	1.79(fixed)	$1.63 \pm 0.40$		4.4/9
powl + powl	1.79(fixed)	$1.04^{+0.57}_{-0.52}$	$4.83^{+1.53}_{-0.56}$	17.2/28
powl + raymond	1.79(fixed)	$1.30^{+0.42}_{-0.43}$	$50^{+15}_{-11}$	16.4/28
powl + zbremss	1.79(fixed)	$1.34^{+0.42}_{-0.40}$	$59^{+26}_{-15}$	16.7/28
powl + zbbdy	$1.1^{+4.2}_{-0.9}$	$1.30^{+0.42}_{-0.64}$	$42^{+41}_{-21}$	16.6/27
powl + zbbdy	1.79(fixed)	$1.37 \pm 0.49$	$32.5^{+8.0}_{-6.0}$	16.9/28
powl + zbbdy (RASS)	1.79(fixed)	$1.47^{+0.77}_{-0.92}$	$30^{+12}_{-10}$	10.7/9
powl + diskbb	$1.2^{+2.5}_{-0.7}$	$1.29^{+0.40}_{-0.66}$	$48^{+53}_{-27}$	16.6/27
powl + diskbb	1.79(fixed)	$1.36 \pm 0.41$	$39.6^{+12.3}_{-7.5}$	16.8/28

<sup>a</sup>Source model (as in XSPEC) modified by neutral absorption (wabs) with column density  $N_{\text{H}}$ : powl – power-law with photon index  $\Gamma$ ; raymond – Raymond-Smith thin plasma emission (abundance fixed at solar); zbremss – redshifted thermal bremsstrahlung; zbbdy – redshifted blackbody with effective temperature  $kT$ ; diskbb – multi-colour disc model with the (rest frame) maximum temperature  $kT$  (see text)

<sup>b</sup> $\Gamma_s$ : photon index of a second softer power-law

<sup>c</sup>the Galactic  $N_{\text{H}}$  value, fixed in fitting

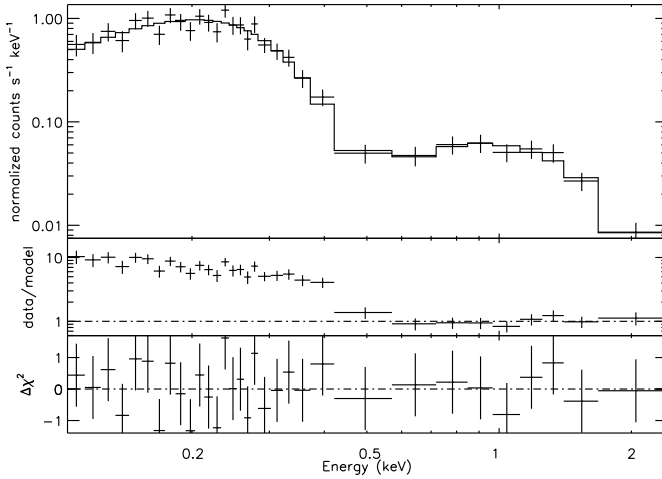


FIG. 1. — Upper panel: *ROSAT* PSPC spectrum of RX J1633+4718 and the best-fit model of a power-law plus a blackbody ( $N_{\text{H}}$  fixed at Galactic  $N_{\text{H}}^{\text{Gal}}$ ). Middle: data to model ratio, where a power-law model with fixed  $N_{\text{H}}^{\text{Gal}}$  is fitted to the 0.5–2.4 keV band and extrapolated down to 0.1 keV. An overwhelming soft X-ray excess is evident. Lower: residuals of the best-fit model as in the upper panel.

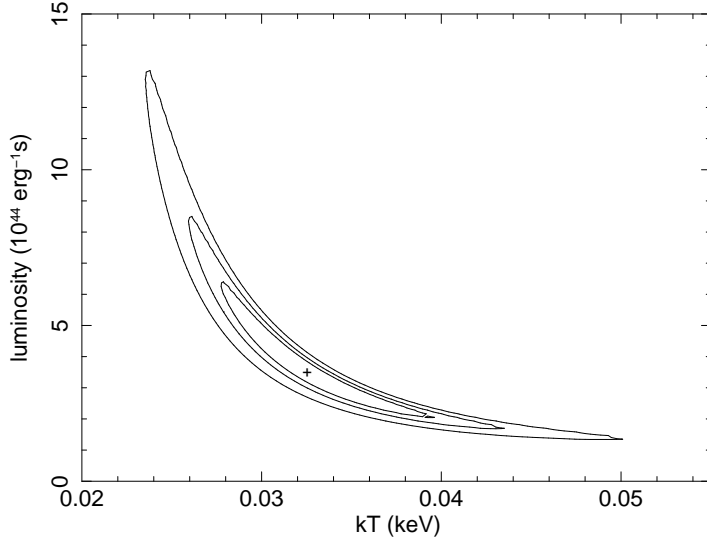


FIG. 2.— Confidence contours (68%, 90%, 99% for two interesting parameters) for the fitted effective temperature and luminosity for the blackbody model component.

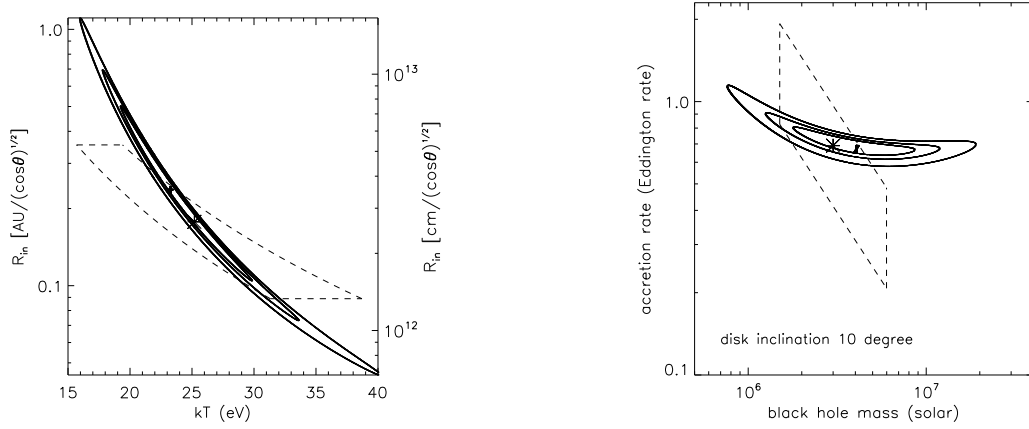


FIG. 3.— Confidence contours (solid; 68%, 90%, 99%) for the maximum effective temperature vs. the inner radius of the disc (left panel) and the BH mass versus scaled accretion rate (right panel; assuming a disc inclination  $\theta = 10^\circ$ ), derived from fitting the spectrum with the MCD plus a power-law model. The estimated values (asterisk) derived from the optical emission line spectrum and their uncertainty ranges are indicated (dashed;  $\pm 0.3$  dex in BH mass and  $\pm 2(1\sigma)$  in the bolometric correction factor are used).

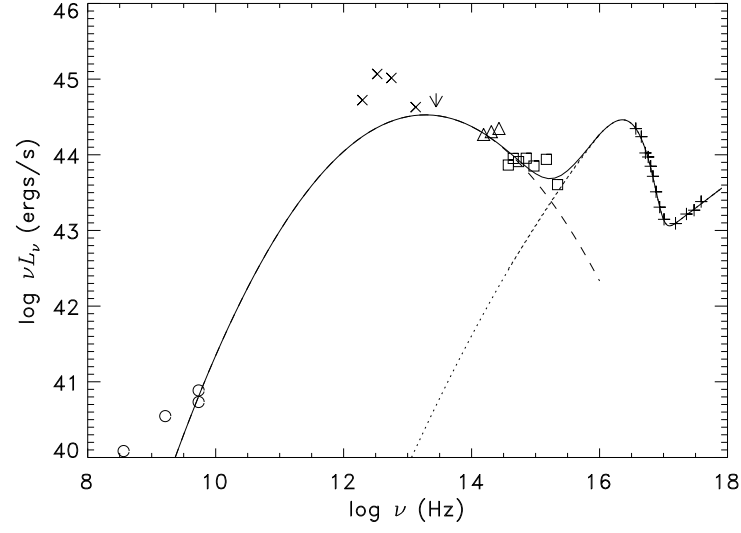


FIG. 4.— Broad-band SED of RX J1633+4718: the unfolded PSPC data (crosses) and the photometric measurements in the UV and optical (*Galex* and SDSS, squares) near-IR (2MASS, triangles), far-infrared (*IRAS* and *ISO*, crosses; arrows indicate upper limits) and radio (circles) bands. The PSF magnitudes are used whenever available. The models are the best-fit MCD+power-law model (dotted), synchrotron emission (dashed) and the sum (solid).